Limits of high-order perturbation theory in time-domain optical mammography

B. Wassermann*
Institut für Experimentalphysik, Free University of Berlin, Arnimallee 14, 14195 Berlin, Germany
and Physikalisch-Technische Bundesanstalt, Abbestrasse 2-12, 10587 Berlin, Germany
(Received 8 March 2006; revised manuscript received 11 May 2006; published 21 September 2006)

Higher order corrections to the Born approximation in perturbation theory are derived in order to improve its performance with the experiments in slablike geometry. A general expression of the *n*th order correction to absorption is developed. The cross talking between absorption and scattering is given. The convergence for higher orders of perturbation analysis for absorbing inclusions was studied. Second order absorption and scattering contributions to the transmitted flux are discussed by analyzing the data from forward simulations. The validity of the results is proven in the experiments with phantoms simulating breast tumors. The significant improvement for the fitted values of the absorption is observed. The alternative application of developed formalism as the first order theory to treat the multiple inclusions is suggested.

DOI: 10.1103/PhysRevE.74.031908 PACS number(s): 87.10.+e, 42.62.Be, 42.25.Dd

I. INTRODUCTION

Applications of optical mammography to tumor diagnostics in the geometry of slightly compressed breast are well documented. Several models were used to analyze the measurements, such as a model of an infinite homogeneous slab [1], photon density waves (PDW) method [1,2], and the random walk approach [3]. However, the application of the PDW method in its present form fails for large objects situated close to the surface of the breast and is restricted to use on spherical targets only, whereas in the random walk analysis a reasonable time effort should be devoted to quantify the exponential correction factor. The homogeneous model, for example, is able to deliver only strongly averaged optical coefficients.

Linear perturbation theory is another method being currently used in practice [4,5]. The general formalism was developed by Arridge *et al.* [6,7]. The necessity of higher order corrections to the Born approximation to improve the perturbation theory for the light distribution in turbid media was outlined by Ostermeyer [8], and Morin *et al.* [9]. Even at moderate values of perturbation, $\delta\mu_a/\mu_{a0}\approx 1$ linear perturbation theory fails to predict the correct optical properties. Recently the use of Padé approximants was proposed by Torricelli *et al.* [10,11] to overcome this problem for the most frequent cases of tumors. However, this empirical method still does not solve the problem for these moderate perturbations ($\delta\mu_a/\mu_{a0}\approx 1$) involving large objects ($\varnothing \geqslant 30$ mm). These deviations are even growing for the cases of reduced absorption and increased scattering, so that the Born approximation turns out here to be a better choice.

Another important issue is the estimate of cross talking between absorption and scattering perturbations. This becomes possible only by using higher orders of perturbation theory. Neither linear perturbation theory nor Padé approximants are taking this nonlinear coupling into account.

Simultaneous treatment of several inclusions presents an unsolved problem in the frame of perturbation theory as well. For the present moment there were no attempts made to describe light transmission through several lesions lying upon each other on the measurement axis.

In the present paper an analytical solution for the leading terms in the Born series is given, since the numerical method of Ostermeyer [8] requires unrealistically large consumption of CPU time resources, huge memory space, and exhausting programming effort. Second and higher Born approximations of perturbation theory are presented. The application of developed formalism as the first order theory for multiple inclusions is discussed. The results are tested on the published experimental data with phantoms [2,12] and compared with those obtained by the method of Padé approximants [10,11].

II. THE THEORY

Diffusion equation is used to describe the light propagation by photons [6]. The system under consideration is a homogeneous slab of thickness d with optical properties, characterized by the absorption (μ_{a0}) and the reduced scattering coefficient (μ'_{s0}). An inclusion with perturbations $\delta\mu_a$ and $\delta\mu'_s$ and volume V_p is embedded in this slab at the position $\vec{r}_p$ from the origin. For simplicity it is assumed that the perturbation is spatially constant across the volume, since the extension to variable perturbations is obvious [13]. Here the diffusion coefficient is chosen to be $D=1/3\mu'_s$ [14]. In this case the Born series is a power series in changes $\delta\mu_a$ of the absorption coefficient and changes of δD.

First of all the expression for total photon density $\phi(\vec{r},t)$ in terms of homogeneous photon density $\phi_0(\vec{r},t)$ and perturbations due the absorption and scattering is considered. The expression for total photon density function $\phi(\vec{r},t)$, given in terms of perturbed photon density operators of Arridge [7], can be casted in the form of the Fredholm equation of the second kind [15].

$$\phi(\vec{r},t) = \phi_0(\vec{r},t) - \delta\mu_a \int G(\vec{r},t;\vec{r}_p,t_p)\phi(\vec{r}_p,t_p)dV_p dt_p - \delta D \int \nabla_p G(\vec{r},t;\vec{r}_p,t_p)\cdot\nabla_p\phi(\vec{r}_p,t_p)dV_p dt_p. \quad (1)$$

*Email address: wasser@physik.fu-berlin.de

The solution can be obtained recursively and is conveniently written in the form of Neumann series. After applying the perturbation theory in the Born approximation, the first correction to total photon density

$$\delta\phi_{tot}^{(1)}(\vec{r},t) = \delta\phi_a^{(1)}(\vec{r},t) + \delta\phi_D^{(1)}(\vec{r},t) \tag{2a}$$

is readily expressed through the absorptive

$$\delta\phi_a^{(1)}(\vec{r},t) = -\,\delta\mu_a \int G(\vec{r},t;\vec{r}_p,t_p)\phi_0(\vec{r}_p,t_p)dV_p dt_p \tag{2b}$$

and scattering component

$$\delta\phi_D^{(1)}(\vec{r},t) = -\,\delta D \int \nabla_p G(\vec{r},t;\vec{r}_p,t_p)\cdot\nabla_p\phi_0(\vec{r}_p,t_p)dV_p dt_p. \tag{2c}$$

Here $G_{slab}(\vec{r},t;\vec{r}_p,t_p)$ denotes the Green's function for the diffusion equation describing the light propagation in a homogeneous medium.

The light propagation in a slab can be described similarly as in an infinite medium, by accounting for the boundary conditions through the introduction of a series of mirror sources and drains [16]. The complete Green's function of the slab is expressed by the sum of the negative and positive imaginary source contributions [6]:

$$G_{slab}(\vec{r},t;\vec{r}_p,t_p) = \sum_{m=-\infty}^{\infty} G[\vec{r},t;\vec{R}_{pm}^{+}(\vec{r}_p,t_p)] - G[\vec{r},t;\vec{R}_{pm}^{-}(\vec{r}_p,t_p)] \tag{3}$$

with the Green's function of a single source in an infinite medium

$$G(\vec{r},t;R_{pm}^{\pm},t_p) = \frac{v}{[4\pi D_0 v(t-t_p)]^{3/2}} \exp\left[-\frac{(\vec{r}-\vec{R}_{pm}^{\pm})^2}{4D_0 v(t-t_p)} - \mu_{a0} v(t-t_p)\right]\theta(t-t_p), \tag{4}$$

where following distances were introduced

$$\vec{R}_{pm}^{+} = \vec{r}_p + 2m(d+2z_e)\vec{e}_z, \tag{5a}$$

$$\vec{R}_{pm}^{-} = \vec{r}_p + 2[m(d+2z_e) - z_e - z_p]\vec{e}_z. \tag{5b}$$

Here, v is the speed of light in the medium of the slab and $\theta(t-t_p)$ is the Heaviside function for the light emitted at time t_p and position $\vec{r}_p$. Distance z_e is incorporated to introduce the extrapolated boundary conditions. It depends on D_0 and refractive index n of the medium and is estimated along the lines of Ref. [17] in the experimental studies described below.

Finally a convenient definition of quantities proportional to the flux transmitted at the exit surface is introduced [17]:

$$\Gamma(\vec{r}_{\det},t;\vec{R}_{pm}^{\pm},t_p) = \left.\frac{\partial G(x,y,z,t;\vec{R}_{pm}^{\pm},t_p)}{\partial z}\right|_{z=d}, \tag{6a}$$

$$\Gamma_{slab}(\vec{r}_{\det},t;\vec{r}_p,t_p) = \sum_{m=-\infty}^{\infty} \Gamma(\vec{r}_{\det},t;\vec{R}_{pm}^{+},t_p) - \Gamma(\vec{r}_{\det},t;\vec{R}_{pm}^{-},t_p). \tag{6b}$$

The distances $r_m^{\pm}$ from the detector at position $\vec{r}_{\det}=(x,y,d)$ to infinite number m of negative and positive sources in (6b) are calculated as the norm of vectors

$$\vec{r}_m^{\pm} = \vec{r}_{\det} - \vec{R}_{pm}^{\pm}. \tag{7}$$

A. Second order correction to absorption term

The second order correction to the absorption term is obtained by substituting the perturbed fluence $\phi_0(\vec{r},t) + \delta\phi_{\rm tot}^{(1)}(\vec{r},t)$ in the expression (2b) instead of the unperturbed $\phi_0(\vec{r},t)$,

$$\delta\phi_a^{(2)}(\vec{r},t) = -\,\delta\mu_a \int_0^t \int_{V_p} G_{slab}(\vec{r},t;\vec{r}_p,t_p)[\phi_0(\vec{r}_p,t_p) + \delta\phi_{tot}^{(1)}(\vec{r}_p,t_p)]dV_p dt_p. \tag{8}$$

After splitting out the term describing the Born approximation

$$\delta\phi_a^{(2)}(\vec{r},t) = \delta\phi_a^{(1)}(\vec{r},t) - \delta\mu_a \int_0^t \int_{V_p} G_{slab}(\vec{r},t;\vec{r}_p,t_p) \times \delta\phi_{tot}^{(1)}(\vec{r}_p,t_p)dV_p dt_p \tag{9}$$

the change in the second order transmitted flux due to absorption can be deduced with the help of Eq. (6a) as

$$\begin{aligned}\delta T_a(x,y,t) &= \delta T_a^{(1)}(x,y,t) + \delta T_a^{(2)}(x,y,t) \\ &= \delta T_a^{(1)}(x,y,t) - \delta\mu_a D_0 \int_0^t \int_{V_p} \Gamma_{slab}(\vec{r}_{\det},t;\vec{r}_p,t_p) \times \delta\phi_{tot}^{(1)}(\vec{r}_p,t_p)dV_p dt_p.\end{aligned} \tag{10}$$

The explicit expressions for the components of $\delta\phi_{\rm tot}^{(1)}(\vec{r}_p,t_p)$ are given by

$$\delta\phi_a{}^{(1)}(\vec{r}_p,t_p) = -\,\delta\mu_a \int_0^{t_p} \int_{V_q} G_{slab}(\vec{r}_p,t_p;\vec{r}_q,t_q) \times G_{slab}(\vec{r}_q,t_q;\vec{r}_0,0)dV_q dt_q, \tag{11a}$$

$$\delta\phi_D^{(1)}(\vec{r}_p,t_p) = -\,\delta D \int_0^{t_p} \int_{V_q} \nabla_q G_{slab}(\vec{r}_p,t_p;\vec{r}_q,t_q)\cdot\nabla_q \times G_{slab}(\vec{r}_q,t_q;\vec{r}_0,0)dV_q dt_q \tag{11b}$$

with source position at $\vec{r}_0=(0,0,z_0)$ and $z_0=1/\mu_{s0}'$. The purely second order contribution $\delta T_a^{(2)}(x,y,t)$, see Eq. (10), actually consists out of two parts itself and can be split into the pure second order absorption contribution

$$\delta T^{(2)}_{abs\text{-}abs}(x,y,t) = -\,\delta\mu_a D_0 \int_0^t \int_{V_p} \Gamma_{slab}(\vec{r}_{\det},t;\vec{r}_p,t_p) \times \delta\phi_a^{(1)}(\vec{r}_p,t_p)dV_p dt_p \tag{12a}$$

and into a cross term, coupling absorption to scattering, the so-called "cross talking"

$$\delta T^{(2)}_{abs\text{-}scat}(x,y,t) = -\,\delta\mu_a D_0 \int_0^t \int_{V_p} \Gamma_{slab}(\vec{r}_{\det},t;\vec{r}_p,t_p) \times \delta\phi_D^{(1)}(\vec{r}_p,t_p)dV_p dt_p. \tag{12b}$$

The expressions in (11a) and (11b) should be then substituted into (12a) and (12b), respectively.

The integrals in Eqs. (12a) and (12b) contain summations for all negative and positive sources for Green's function $G_{slab}(\vec{r},t;\vec{r}_p,t_p)$, see Eq. (3). Here an explicit form for an arbitrary term entering such a sum in the pure second order absorption correction to transmitted flux, given in (12a), is shown

$$J^{\alpha\beta\gamma(2)}_{m,n,k_{abs\text{-}abs}} = -\,(\delta\mu_a)^2 D_0 \int_0^t \int_{V_p} dV_p dt_p \Gamma(\vec{r}_{\det},t;\vec{R}^{\alpha}_{pm},t_p) \times \int_0^{t_p} \int_{V_q} dV_q dt_q G(\vec{r}_p,t_p;\vec{R}^{\beta}_{qn},t_q) G(\vec{r}_q,t_q;\vec{R}^{\gamma}_{0k},0), \tag{13}$$

where vectors sets $\vec{r}^{\pm}_{pn}$, $\vec{r}^{\pm}_{qk}$, and $\vec{R}^{\pm}_{qn}$ and $\vec{R}^{\pm}_{0k}$ are defined similarly to Eqs. (5) and (7),

$$\vec{r}^{+}_{pn} = \vec{r}_p - \vec{R}^{+}_{qn} = \vec{r}_p - [\vec{r}_q + 2n(d+2z_e)\vec{e}_z], \tag{14a}$$

$$\vec{r}^{-}_{pn} = \vec{r}_p - \vec{R}^{-}_{qn} = \vec{r}_p - \{\vec{r}_q + 2[n(d+2z_e) - z_e - z_q]\vec{e}_z\}, \tag{14b}$$

$$\vec{r}^{+}_{qk} = \vec{r}_q - \vec{R}^{+}_{0k} = \vec{r}_q - [\vec{r}_0 + 2k(d+2z_e)\vec{e}_z], \tag{14c}$$

$$\vec{r}^{-}_{qk} = \vec{r}_q - \vec{R}^{-}_{0k} = \vec{r}_q - \{\vec{r}_0 + 2[k(d+2z_e) - z_e - z_0]\vec{e}_z\}. \tag{14d}$$

The sign indices α, β, and γ are either equal to 0 or 1 for positive and negative subscripts, respectively. Figure 1(a) shows the geometrical configuration of the model and distances introduced in Eqs. (5), (7), and (14).

By inserting the explicit form of the integrand in Eq. (13), using the definition of the Green's function given by (4), one faces the calculation of a double time integral

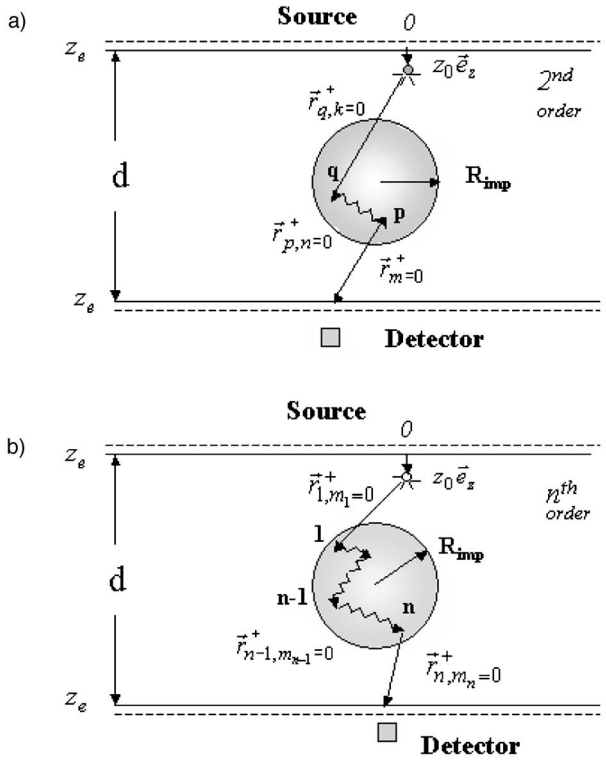

FIG. 1. (a) Geometry of the second order perturbation theory for a spherical inclusion with radius R_{imp} embedded in a homogeneous slab of thickness d; z_e is the distance to the extended boundary; the source is at distance z_0 below the origin 0; (b) same picture in the case of the nth order theory. The wavy lines are connecting points of different scattering events. Cases with $m_p \neq 0$ relating to the mirror imaged spheres are not shown in this picture.

$$J^{\alpha\beta\gamma(2)}_{m,n,k_{abs\text{-}abs}} = -\,(\delta\mu_a)^2 \frac{\exp(-\mu_{a0}vt)}{(4\pi)^{9/2}D_0^{7/2}v^{3/2}} \frac{\partial}{\partial z} \int_0^t \int_{V_p} dV_p dt_p \times \frac{\exp\left[-\dfrac{r_m^{\alpha 2}}{4D_0v(t-t_p)}\right]}{(t-t_p)^{3/2}} \int_0^{t_p} \int_{V_q} dV_q dt_q \times \frac{\exp\left[-\dfrac{r_{pn}^{\beta 2}}{4D_0v(t_p-t_q)} - \dfrac{r_{qk}^{\gamma 2}}{4D_0vt_q}\right]}{(t_p-t_q)^{3/2}t_q^{3/2}}. \tag{15}$$

The coupling of absorption to scattering is deduced similarly

$$J^{\alpha\beta\gamma(2)}_{m,n,k_{abs\text{-}scat}} = -\,\delta\mu_a \delta D D_0 \int_0^t \int_{V_p} dV_p dt_p \Gamma(\vec{r}_{\det},t;\vec{R}^{\alpha}_{pm},t_p) \times \int_0^{t_p} \int_{V_q} dV_q dt_q \nabla_q G(\vec{r}_p,t_p;\vec{R}^{\beta}_{qn},t_q)\cdot\nabla_q \times G(\vec{r}_q,t_q;\vec{R}^{\gamma}_{0k},0) \tag{16}$$

and explicitly

$$J^{\alpha\beta\gamma(2)}_{m,n,k_{abs\text{-}scat}} = \delta\mu_a \delta D \frac{\exp(-\mu_{a0} v t)}{4(4\pi)^{9/2} D_0^{11/2} v^{7/2}} \frac{\partial}{\partial z} \int_0^t \int_{V_p} dV_p dt_p \times \frac{\exp\left[-\frac{r_m^{\alpha 2}}{4D_0 v(t-t_p)}\right]}{(t-t_p)^{3/2}} \int_0^{t_p} \int_{V_q} dV_q dt_q \times \frac{\vec{\vec{r}}^{\,*}_{pq} \exp\left[-\frac{r_{pn}^{\beta 2}}{4D_0 v(t_p-t_q)} - \frac{r_{qk}^{\gamma 2}}{4D_0 v t_q}\right]}{(t_p-t_q)^{5/2} t_q^{5/2}}. \quad (17)$$

The scalar product $\vec{\vec{r}}^{\,*}_{pq} = \vec{r}^{\,*\beta}_{pn} \cdot \vec{r}^{\,\gamma}_{qk}$ depends on the sign β of the imaginary source through the definition $\vec{r}^{\,*\beta}_{pn} = \{x_{pn}, y_{pn}, (-1)^\beta z_{pn}\}$. The temporal integrals can be calculated explicitly as described in Appendix B.

B. Second order correction to scattering term

The second order contribution to scattering is constructed in the same fashion from Eq. (2c). By omitting some redundant steps close to the derivation performed in Eqs. (8)–(11), one arrives at expressions similar to (12). The coupling of scattering to absorption delivering the second part of the "cross talking" is given by

$$\delta T^{(2)}_{scat-abs}(x,y,t) = -\delta D D_0 \int_0^t \int_{V_p} \nabla_p \Gamma_{slab}(\vec{r}_{\text{det}}, t; \vec{r}_p, t_p) \cdot \nabla_p \delta\phi^{(1)}_a(\vec{r}_p, t_p) dV_p dt_p \quad (18a)$$

whereas the last contribution responsible for the second order scattering correction can be written

$$\delta T^{(2)}_{scat-scat}(x,y,t) = -\delta D D_0 \int_0^t \int_{V_p} \nabla_p \Gamma_{slab}(\vec{r}_{\text{det}}, t; \vec{r}_p, t_p) \cdot \nabla_p \delta\phi^{(1)}_D(\vec{r}_p, t_p) dV_p dt_p. \quad (18b)$$

After substituting the expressions of $\delta\phi^{(1)}_a(\vec{r}_p, t_p)$ and $\delta\phi^{(1)}_D(\vec{r}_p, t_p)$ given in (11) into Eq. (18a) and differentiating, one gets the following expression for summation in the case of scattering-absorption interaction:

$$J^{\alpha\beta\gamma(2)}_{m,n,k_{scat\text{-}abs}} = -\delta\mu_a \delta D D_0 \int_0^t \int_{V_p} dV_p dt_p \nabla_p \Gamma(\vec{r}_{\text{det}}, t; \vec{R}^{\alpha}_{pm}, t_p) \cdot \int_0^{t_p} \int_{V_q} dV_q dt_q [\nabla_p G(\vec{r}_p, t_p; \vec{R}^{\beta}_{qn}, t_q)] \times G(\vec{r}_q, t_q; \vec{R}^{\gamma}_{0k}, 0). \quad (19)$$

Consequently

$$J^{\alpha\beta\gamma(2)}_{m,n,k_{scat\text{-}abs}} = \delta\mu_a \delta D \frac{\exp(-\mu_{a0} v t)}{4(4\pi)^{9/2} D_0^{11/2} v^{7/2}} \frac{\partial}{\partial z} \int_0^t \int_{V_p} dV_p dt_p \times \frac{\exp\left[-\frac{r_m^{\alpha 2}}{4D_0 v(t-t_p)}\right]}{(t-t_p)^{5/2}} \int_0^{t_p} \int_{V_q} dV_q dt_q \times \frac{\vec{\vec{r}}^{\,*}_{pm} \exp\left[-\frac{r_{pn}^{\beta 2}}{4D_0 v(t_p-t_q)} - \frac{r_{qk}^{\gamma 2}}{4D_0 v t_q}\right]}{(t_p-t_q)^{5/2} t_q^{3/2}} \quad (20)$$

with scalar product $\vec{\vec{r}}^{\,*}_{pm} = \vec{r}^{\,\beta}_{pn} \cdot \vec{r}^{\,*\alpha}_{m}$, defining $\vec{r}^{\,*\alpha}_m = \{x_m, y_m, (-1)^\alpha z_m\}$ and using $\vec{r}^{\,\beta}_{pn}$ already defined in Sec. II A.

For the case of second order scattering events

$$J^{\alpha\beta\gamma(2)}_{m,n,k_{scat\text{-}scat}} = -(\delta D)^2 \cdot D_0 \int_0^t \int_{V_p} dV_p dt_p \nabla_p \Gamma(\vec{r}_{\text{det}}, t; \vec{R}^{\alpha}_{pm}, t_p) \cdot \nabla_p \int_0^{t_p} \int_{V_q} dV_q dt_q [\nabla_q G(\vec{r}_p, t_p; \vec{R}^{\beta}_{qn}, t_q) \cdot \nabla_q G(\vec{r}_q, t_q; \vec{R}^{\gamma}_{0k}, 0)] \quad (21)$$

and in the same spirit as before

$$J^{\alpha\beta\gamma(2)}_{m,n,k_{scat\text{-}scat}} = (\delta D)^2 \frac{\exp(-\mu_{a0} v t)}{8(4\pi)^{9/2} D_0^{13/2} v^{9/2}} \frac{\partial}{\partial z} \int_0^t \int_{V_p} dV_p dt_p \times \frac{\exp\left[-\frac{r_m^{\alpha 2}}{4D_0 v(t-t_p)}\right]}{(t-t_p)^{5/2}} \int_0^{t_p} \int_{V_q} dV_q dt_q \times \left[\vec{\vec{r}}^{\,**}_{qm} - \frac{\vec{\vec{r}}^{\,*}_{pq} \vec{\vec{r}}^{\,*}_{pm}}{2D_0 v(t_p-t_q)}\right] \times \frac{\exp\left[-\frac{r_{pn}^{\beta 2}}{4D_0 v(t_p-t_q)} - \frac{r_{qk}^{\gamma 2}}{4D_0 v t_q}\right]}{(t_p-t_q)^{5/2} t_q^{5/2}}, \quad (22)$$

where $\vec{\vec{r}}^{\,**}_{qm} = \vec{r}^{\,*\alpha}_m \cdot \vec{r}^{\,**\gamma}_{qk}$; and importantly $\vec{r}^{\,**\gamma}_{qk} = \{x_{qk}, y_{qk}, (-1)^\beta z_{qk}\}$ is marked by a double star, since the sign of its z component depends on β and not on γ as it might be expected here!

Now, keeping in mind the sign ordering in expression (3), one can write the summations for any of the four terms above in a general form

$$\delta T^{(2)}(x,y,t) = \sum_{\alpha,\beta,\gamma=0,1} \sum_{m,n,k=-\infty}^{\infty} (-1)^{\alpha+\beta+\gamma} J^{\alpha\beta\gamma(2)}_{m,n,k}. \quad (23)$$

The explicit form of $\delta T^{(2)}(x,y,t)$ for all four types of second order correction to perturbation theory is given in Appendix A, by Eqs. (A3)–(A6). The derivation of time integrals entering the expressions (15), (17), (20), and (22) is shown in Appendix B. All definitions of distances and scalar products of spatial vectors used in this work are summarized in Table I. The flux of transmitted photons is then calculated as the sum $T^{(0)} + \delta T^{(1)} + \delta T^{(2)}$ where the first two terms are well

TABLE I. Notations of the distances, vectors or their dot products.

Abbreviation used for distances, vectors, or scalar products		
	1st and 2nd Order	nth Order
$\vec{r}_m^{*\alpha}$	$\{x_m, y_m, (-1)^\alpha z_m\}$	$\vec{R}^+_{p,m_p}=\vec{r}_p+2m_p(d+2z_e)\vec{e}_z;$
$\vec{r}_{pn}^{*\beta}$	$\{x_{pn}, y_{pn}, (-1)^\beta z_{pn}\}$	$\vec{R}^-_{p,m_p}=\vec{r}_p+2[m_p(d+2z_e)-z_e-z_p]\vec{e}_z;$
$\vec{r}_{qk}^{**\gamma}$	$\{x_{qk}, y_{qk}, (-1)^\beta z_{qk}\}$	$\vec{r}^{\pm}_{p,m_p}=\vec{r}_{p+1}-\vec{R}^{\pm}_{p,m_p}$
$\vec{r}_{qk}^{*\gamma}$	$\{x_{qk}, y_{qk}, (-1)^\gamma z_{qk}\}$	with $p=0,\ldots n$; $m_p=-\infty,\ldots,\infty$
	$\vec{r}_{pn}^{*\beta}\cdot\vec{r}_{qk}^{\gamma}$	$\vec{r}_{n+1}=\vec{r}_{\mathrm{det}}$
	$\vec{r}_{pn}^{\beta}\cdot\vec{r}_m^{*\alpha}$	
	$\vec{r}_{qm}^{\gamma}\cdot\vec{r}_m^{*\alpha}$	
$\overleftrightarrow{r}_{qm}^{**}$	$\vec{r}_{qk}^{**\gamma}\cdot\vec{r}_m^{*\alpha}$	note that in second order
	$\vec{r}_{pn}^{\beta}\cdot\vec{r}_m^{*\alpha}$	$\vec{r}_q$ and $\vec{r}_p$ for $\vec{r}_{p=1}$ and $\vec{r}_{p=2}$
		m, n, k for m_2, m_1, m_0
$r^{\pm}_{qm}$	$r_m^\alpha \pm r_{qk}^\gamma$	$\vec{r}^{\pm}_j=\vec{r}_{\mathrm{det}}-\vec{R}^{\pm}_{pj}$; $j=n,m,k$
$r^{\times}_{qm}$	$r_m^\alpha \cdot r_{qk}^\gamma$	
$r^{\pm}_{pq}$	$r_{pn}^\beta \pm r_{pq}^\gamma$	
r_{pqm}	$r^+_{pq}+r^\alpha_m$	
$r^{\times}_{pq}$	$r_{pn}^\beta \cdot r_{qk}^\gamma$	

known from the Born approximation [5], explicitly given by (A1) and (A2) in Appendix A.

For higher orders special care should be taken to handle the singularity in the kernel. The procedure, similar to the one given in [8], is described in Sec. II D, followed by the convergence analysis of the Born perturbation series.

C. General form of the correction to absorption

In the same spirit one can continue the iteration to deduce the general expression to the nth order correction to pure absorption, the case important for most tumors. By looking at the analytical form for the photon density in the first, second, third, and fourth Born approximations (last two omitted here for the sake of simplicity) one can deduce the general expression for the nth term

$$I^{(n)}_{m_0,\ldots,m_n}{}^{\alpha_0,\ldots,\alpha_n} = \frac{e^{-\mu_a ct}}{(4\pi D_0 t)^{3/2}\sqrt{v}}\left(\frac{-\delta\mu_a}{4\pi D_0}\right)^n \int_{V_1}\cdots\int_{V_i} \cdots \int_{V_n} \frac{\sum_{p=0}^{n} r^{\alpha_p}_{p,m_p}}{\prod_{p=0}^{n} r^{\alpha_p}_{p,m_p}} \exp\left[-\frac{\left(\sum_{p=0}^{n} r^{\alpha_p}_{p,m_p}\right)^2}{4D_0 vt}\right] d^nV, \tag{24}$$

$$\delta\phi^{(n)}_a(x,y,t) = \sum_{\alpha_0,\ldots,\alpha_n=0,1}\ \sum_{m_0,\ldots,m_n=-\infty}^{\infty} (-1)^{\alpha_0+\ldots+\alpha_n} I^{(n)}_{m_0,\ldots,m_n}{}^{\alpha_0,\ldots,\alpha_n}. \tag{25}$$

The expression for flux $J^{(n)}_{m_0,\ldots,m_n}{}^{\alpha_0,\ldots,\alpha_n} = -D_0\frac{\partial}{\partial z} I^{(n)}_{m_0,\ldots,m_n}{}^{\alpha_0,\ldots,\alpha_n}$ should be substituted in a formula similar to (25)

$$\delta T^{(n)}_{abs}(x,y,t) = \sum_{\alpha_0,\ldots,\alpha_n=0,1}\ \sum_{m_0,\ldots,m_n=-\infty}^{\infty} (-1)^{\alpha_0+\ldots+\alpha_n} J^{(n)}_{m_0,\ldots,m_n}{}^{\alpha_0,\ldots,\alpha_n} \tag{26}$$

to obtain the nth order transmission.

$$J^{(n)}_{m_0,\ldots,m_n}{}^{\alpha_0,\ldots,\alpha_n} = \frac{e^{-\mu_a ct} D_0}{(4\pi D_0 t)^{3/2}\sqrt{v}}\left(\frac{-\delta\mu_a}{4\pi D_0}\right)^n \int_{V_1}\cdots\int_{V_i} \cdots \int_{V_n} \frac{z^{\alpha_n}_{m_n}}{r^{\alpha_n}_{m_n}\prod_{p=0}^{n} r^{\alpha_p}_{p,m_p}} \left[\frac{\sum_{p=0}^{n-1} r^{\alpha_p}_{p,m_p}}{r^{\alpha_n}_{m_n}} + \frac{\left(\sum_{p=0}^{n} r^{\alpha_p}_{p,m_p}\right)^2}{2D_0 vt}\right] \times \exp\left[-\frac{\left(\sum_{p=0}^{n} r^{\alpha_p}_{p,m_p}\right)^2}{4D_0 vt}\right] d^nV \tag{27}$$

where for the sake of generality $\vec{r}^{\alpha_p}_{p,m_p}$ is the vector connecting the source to every single event in the multiple absorption chain on the way to detector, see Fig. 1(b). Index set p,m_p points at the absorption event in a sphere considered for the pth order interaction contributing to the nth order of perturbation; the inhomogeneity is formally reflected m_p- or (m_p+1) times at the slab boundary. The double-valued index α_p (0 or 1) is used to distinguish the positive and negative sources. Except for the first and last terms, the general form of $\vec{r}^{\alpha_p}_{p,m_p}$ is reflected by $\vec{r}^{\pm}_{pn}$ in Eqs. (14a) and (14b). As for first term, $\vec{r}^{\alpha_0}_{p=0,m_0}$ is the vector linking the first inhomogeneity to the source, similarly to $\vec{r}^{\pm}_{qk}$ in Eqs. (14c) and (14d). In turn the last term, $\vec{r}^{\alpha_n}_{n,m_n}$, links the last, nth inhomogeneity to detector and is identical to $\vec{r}^{\pm}_m$, Eqs. (5) and (7). A full diagram-

matic analysis of formula (27) certainly presents an attractive goal for future research.

D. The calculation of absorption in the singular region and convergence criterion

As an example let us consider a spherical inhomogeneity with radius R_{imp}. The integral in Eq. (24) can be rewritten as

$$I_{m_0,\ldots,m_n}^{\alpha_0,\ldots,\alpha_n\ (n)} = \frac{e^{-\mu_a c t}}{(4\pi D_0 t)^{3/2}\sqrt{v}}\left(\frac{-\delta\mu_a}{4\pi D_0}\right)^n \int_{V_1}\cdots\int_{V_i} \cdots \int_{V_n}\left(\sum_{i=1}^{n}\frac{1}{\prod_{p\neq i}^{n} r_{p,m_p}^{\alpha_p}}\right)\exp\left(-\frac{\left(\sum_{p=0}^{n} r_{p,m_p}^{\alpha_p}\right)^2}{4D_0 v t}\right) d^n V. \tag{28}$$

Each of n terms of the sum in has a singularity of order n -1 provided all interactions are in the same sphere. This is the case shown in Fig. 1(b). Following the method outlined by Ostermeyer [8] one can replace the integration over a Cartesian voxel possessing this singularity through integration over a sphere with volume equal to the voxel volume. The radius ε of such a sphere is thus proportional to the size of the voxel R_{imp}/N with N^3 being the total number of voxels,

$$\varepsilon = \sqrt[3]{\frac{3}{4\pi}}\frac{R_{imp}}{N}.$$

By considering every single integration volume $p\neq i$ and omitting subscripts for the sake of simplicity one can express every single integral over $V_{p,m}$ as

$$I_{p,p-1} = \int_V \frac{dV_{p,m}}{r_{p,m} r_{p-1,m}} = \int_V \frac{dV_p}{|\vec{r}_{p+1}-\vec{r}_p||\vec{r}_p-\vec{r}_{p-1}|}$$

with setting the exponential term to its maximum value 1. In the case of the second order $\vec{r}_{p+1}\neq\vec{r}_{p-1}$, being distances to the real detector and source, respectively. Hence the integral over this voxel can be done directly in spherical coordinates by translating the origin to its center and it turns out to be proportional to $2\pi\varepsilon^2$.

Since for the nth order this condition is no more valid, one can get an estimate of $I_{p,p-1}$ in terms of beta functions, by integrating it in Cartesian coordinates, along the lines of Morse and Feshbach (MF), Ref. [18] (see also Appendix C). With the help of (C3), Eq. (28) reduces to

$$\begin{aligned} I_{m_0,\ldots,m_n}^{\alpha_0,\ldots,\alpha_n\ (n)} &\leqslant \frac{e^{-\mu_a c t}}{(4\pi D_0 t)^{3/2}\sqrt{v}}\left(\frac{|\delta\mu_a|}{4\pi D_0}\right)^n \sum_i^n \int_{V_1}\frac{dV_1}{r_{1,m_1}^{\alpha_1}}\cdots \\ &\times \int_{V_{p\neq i}}\frac{dV_{p\neq i}}{r_{p\neq i,m_{p\neq i}}^{\alpha_i}}\cdots\int_{V_n}\frac{dV_n}{r_{n,m_n}^{\alpha_n}} \\ &\leqslant \frac{e^{-\mu_a c t}}{(4\pi D_0 t)^{3/2}\sqrt{v}}\left(\frac{|\delta\mu_a|}{4\pi D_0}\right)^n C(2\varepsilon)^{2n}, \end{aligned} \tag{29}$$

where C is an integration constant.

Finally, the Cauchy condition for the convergence of Born series is approximately expressed through

$$\frac{|\delta\mu_a|R_{imp}^2}{\pi N^2 D_0} = \frac{\Lambda}{\pi N^2} \leqslant 1. \tag{30}$$

Formula (29) is a recipe to handle the nth order singularity in absorption expression—an alternative to the method outlined by Ostermeyer in [8] for solutions of Helmholtz equation. For the typical values $\delta\mu_a=0.08\ \mathrm{cm}^{-1}$, $D_0=0.03$ cm, and discretization value of say $N=14$, the critical value of R_{imp} is far away from raising convergence problems in absorption of any order. Here we introduce the dimensionless characteristic parameter

$$\Lambda = \frac{|\delta\mu_a|R_{imp}^2}{D_0}$$

providing a qualitative physical criterion for a perturbation approach. One can immediately realize, that this characteristic perturbation parameter Λ in Eq. (30) is nothing else as twice the index of the exponential correction factor in the random walk theory of Ref. [3], pointing at the remarkable correlation between these two theories.

By analyzing the second order scattering term, Eq. (A6), it becomes clear that terms containing $(r_{pn}^{\beta})^5$ in the denominator would lead to logarithmic singularity of the form

$$\int_0^{\varepsilon}\frac{f(r_{pn}^{\beta})}{r_{pn}^{\beta}}dr_{pn}^{\beta}$$

unavoidably resulting in divergence of a Neumann series. Here, $f(r_{pn}^{\beta})$ is analytic and bound in the integration range. On the other hand, the condition δD to be taken constant within the impurity imposes a constant number of scatterers separated by a minimal distance of several diffusion lengths $\left(\frac{1}{3\mu_{s0}'}\right)$. This argument allowed us to set a lowest integration limit in formula (A6), preventing therewith any problems with singular behavior of the integrand and "self-interaction" terms. The stability of the integrand down to the voxel sizes of 1 mm^3 was also verified, and there were no problems encountered. For distances below this minimal limit, the diffusion approximation breaks down and the Born approximation of the Boltzmann radiative transfer equation given in work [19] could be used for estimates. This model accounts for the nearly ballistic motion of photons at early times, contributing equally for tumors and for the homogeneous region.

III. RESULTS AND DISCUSSION

A. Forward calculations of shape functions

Formulas (A3)–(A6) (Appendix A), emerging from the previous Sec. II, are aimed to resolve two important problems. First, as mentioned previously, moderately large perturbations in optical properties ($\delta\mu_a=0.05\ \mathrm{cm}^{-1}$ and $\delta\mu_s'=3-5\mathrm{cm}^{-1}$) are not sufficiently accurately described by the linear perturbation theory at the typical tumor sizes of $R=10$ mm. For tumors with bigger sizes the situation is getting even much worth, so that higher order corrections, particularly in absorption, are needed to improve the fit precision

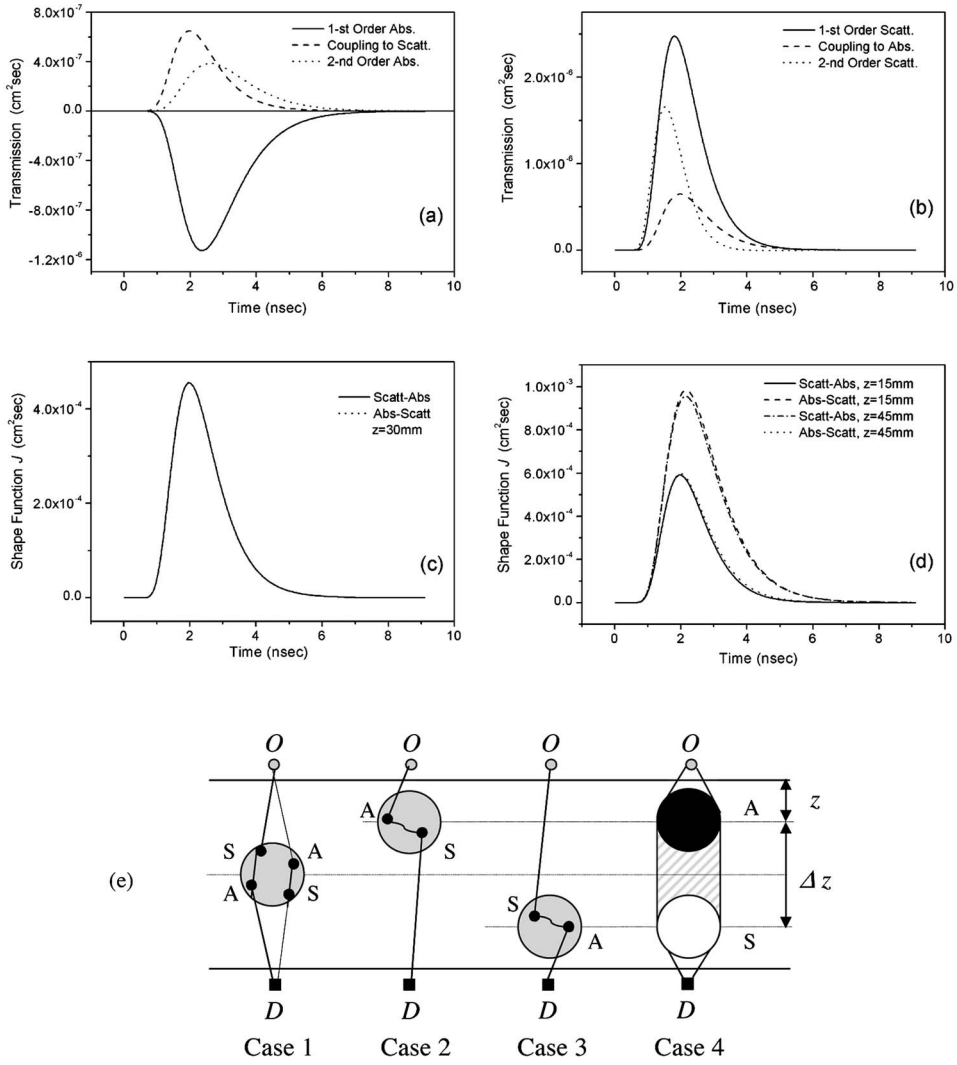

FIG. 2. Higher order perturbation calculations on spherical inhomogeneity with $R=10$ mm, placed in depth z of a $d=60$ mm thick slab with optical coefficients $\mu'_{s0}=10.75\ \mathrm{cm}^{-1}$ and $\mu_{a0}=0.045\ \mathrm{cm}^{-1}$. (a) Comparison of the first and second order absorption contributions to transmission, case $\delta\mu_a=0.046\ \mathrm{cm}^{-1}$, $z=30$ mm; (b) first and second order scattering contributions to transmission, case reduced scattering $\delta\mu'_s=-5.4\ \mathrm{cm}^{-1}$, $z=30$ mm; (c) cross-talk shape functions, $J_{abs\text{-}scat}$ and $J_{scat\text{-}abs}$, calculated from (A3) and (A4), for the middle of the slab, $z=30$ mm. No significant difference can be detected; (d) Same as (c) but for depths $z=15$ mm and $z=45$ mm, reflecting symmetric displacements from the slab midline. (e) Schematic illustration of the time reversibility of perturbation solution to diffusion equation (equivalence to geometrical optics). S stands for the scattering, and A for the absorbing event.

(see Sec. III B below). Figures 2(a) and 2(b) show the forward calculations of various contributions to time-dependent transmission for the typical perturbations mentioned above. In the absorptive case the second order transmission reaches the 35% level of the first order, whereas the cross talk to scattering delivers almost 60% [Fig. 2(a)]. The second order scattering contribution proves to be 70% from its first order, and the cross talk to absoption amounts to 26%.

Another interesting feature observed is the time reversibility of the perturbation solution within the limits of $<1\%$, pointing out the compatibility with geometrical optics. This observation is expected from the reciprocity condition of the Green's function for diffusion, where the involved time reversal is satisfying the causality condition $G(\vec{r},t|\vec{r}_0,t_0)=0$ for $t<t_0$, and homogeneous boundary conditions, see Ref. [18] (MF). Obviously, the small discrepancy is due to the asymmetry between the source positioned at a distance r_0 from the boundary and the detector being placed directly at the edge. Anyway, for a perturbing sphere positioned in the middle of the slab there is *practically no difference* between the cross talks of absorption to scattering, calculated from Eq. (A4) and vice versa—scattering to absorption from (A5), see Fig. 2(c). Schematically this situation is reflected in Fig. 2(e) as case 1. It means also that one needs to calculate only one of these contributions for practical needs; (A4) and (A5) are given here both solely for validation reason. By moving the test object to a certain distance, z close to the source, case 2 in Fig. 2(e), the absorption to scattering coupling becomes almost identical with the scattering to the absorption event occurring at the same distance z from the detector—case 3, in the same figure. The time dependent transmission curves in Fig. 2(d) are reflecting this observation.

This leads us to the second important application for the formalism given by Eqs. (A3)–(A6) as well as by Eq. (27). From cases 2 and 3 shown in Fig. 2(e) differences of about 40–50% are deduced by comparing scattering-absorption (absorption-scattering) events occurring either in the upper or lower parts of the slab, see Fig. 2(d). Now, by separating the z position of the centers of integration volumes V_p and V_q by some Δz, two and more different lesions located along the source-detector axis can be modeled, see case 4 in Fig. 2(e). Here, particular sensitivity for the cross-talk terms to the relative depth difference between the lesions is expected. Total transmission change $T_{total}(t)$ in this case is expressed through the sum of first order perturbation contributions of both lesions, and the perturbation of the light passed through

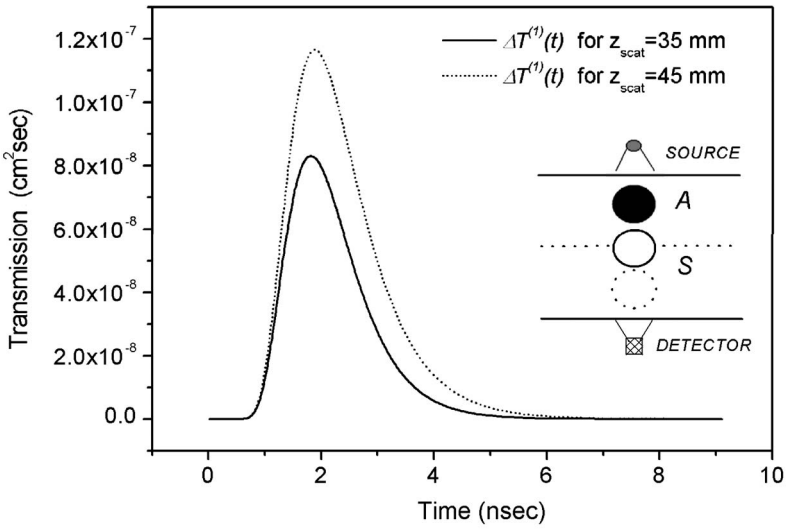

FIG. 3. Depth difference sensitivity of the perturbation method after Eq. (31) [case 4 in Fig. 2(e)] applied to the coaxially placed absorber and scatterer. Solid transmission curve corresponds to the absorber-scatterer depth difference $\Delta z=20$ mm; dotted curve to the depth difference of $\Delta z=30$ mm.

the first sphere (A for absorbing) by the second sphere (S for scattering)

$$\Delta T_{total}(t) = \Delta T^{(1)}_{abs}(z_{abs},t) + \Delta T^{(1)}_{scat}(z_{scat},t) + \Delta T^{(2)}_{abs\text{-}scat}(z_{abs},z_{scat},t), \quad (31)$$

where $\Delta T^{(1)}_{abs}$ and $\Delta T^{(1)}_{scat}$ are the well-known first order contributions of both spheres from (A1) and (A2), Appendix A, located at z_{abs} and at $z_{scat}=z_{abs}+\Delta z$, respectively, and $\Delta T^{(2)}_{abs\text{-}scat}$ is the cross-link term from (A4), but with Δz-displaced positions of integration volumes V_p and V_q.

Figure 3 shows the comparison of two different distances between absorbing and scattering spheres. A quite impressive difference in transmission of about 40% guarantees the sufficient on-axis lesion resolution. The general formalism of Eq. (A3) can be certainly applied for two absorbing lesions, and that of Eq. (A6)—for two scattering lesions as well. Certainly, one should take care to avoid the confusion due to time reversibility of the solution in the coaxial source-detector case. Some additional information to determine the sequence order of lesions is then needed.

B. Comparison with experiments

The experiments on spherical perturbations, having three different radius values 5, 10, and 15 mm, were extensively discussed in Ref. [2]. It should be briefly mentioned that samples were casted by injecting the liquid 3% agarose in water solution in specially designed forms. The scattering properties of the samples were controlled by the amount of the 500 nm sized quartz beads added to the agarose solution. The absorption of the phantoms μ_a was adjusted by the amount of black India ink added to the solution. For reference purposes a slab of the same material was cast in an $8\times8\times3$ cm^3 cuboid shape to determine the optical properties independently by using the model of the homogeneous infinite slab.

The apparatus for measurements at $\lambda=785$ nm with a mode locked Ti:sapphire laser system was described in Ref. [20]. The phantom spheres were immersed in a milk-water-ink solution suited to reproduce the average value $\mu_s'=10$ cm^{-1} typical for the human breast. Spheres were placed in two positions, in the middle of the cuvette (thickness $d=6$ cm) and close to the boundary, hanging on a stretched nonabsorbing fiber. The transmitted distribution of times of flight of photons (DTOF) was measured with a fast photomultiplier and time correlated single photon counting. The measured instrument response [typical full width half maximum (FWHM) 200 ps] was convoluted with calculated DTOFs for fitting experimental data.

In Fig. 4(a) the fit results for different models for a given sample set as a function of the sphere radius are plotted. The starting fit values of optical coefficients are $\mu_{s0}'=9.9$ cm^{-1} ($D_0=0.034$ cm^{-1}) and $\mu_{a0}=0.042$ cm^{-1} for the milk suspension. The absorption coefficient $\mu_a=0.087$ cm^{-1} measured for the reference slab is indicated as a horizontal dotted line. As one can readily see, the best agreement is achieved at the smallest sphere radius 5 mm. For comparison, the results obtained by the diffraction model with the photon density waves (DPDW) [2] method are also shown as solid squares. All models (except of photon density waves, PDW) are giving almost the same value of μ_a, deviating no more than 5–6% from the reference value measured on the reference slab. The situation is getting much worse as one proceeds to the sphere with radius 10 mm, size typical for tumors analyzed in Ref. [20]. The result of the first order perturbation theory is already 15% lower as the reference value, whereas the second order correction is bringing the total μ_a value to fit the reference almost exactly. The PDW method for this case is not the best solution (+15%). In contrast the empirical method of Padé approximants still holds. For the largest sample, having a radius of 15 mm, the linear perturbation theory simply fails with a result of 23% underestimating the expected value. The Padé approximants here tend to overestimate the reference value to about 10–12%. Second order theory improves this value to a deviation of less than 9%, when compared to the experiment. The superior accuracy of the PDW method demonstrated in Ref. [2] is based on the fit to the finite-element method (FEM) calculations as a reference and is not substantiated by the fit to experimental results presented above.

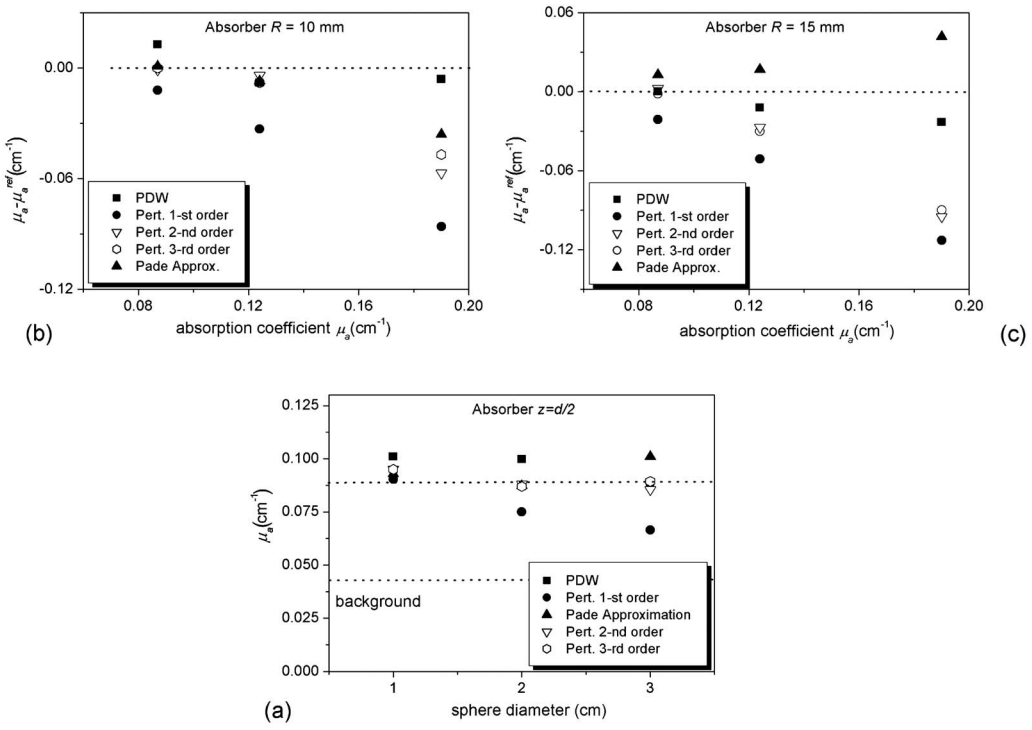

FIG. 4. (a) Absorption coefficients μ_a of agarose spheres with the same ink concentration, obtained by fitting with the help of different approximations of perturbation theory and photon density wave method (PDW) as a function of sphere radius (D_0=0.034 cm^{-1}, μ_{a0}=0.04 cm^{-1}, $\delta\mu_a$=0.045 cm^{-1}); (b) deviation of absorption coefficients μ_a of phantoms from the values μ_a^{ref} of the reference slab as a function of growing absorption μ_a^{ref} (sphere with a frequent tumor radius R_{imp}=10 mm); (c) same for the case R_{imp}=15 mm. Value for the reference slab, μ_a=0.087 cm^{-1}, is shown with a dashed line.

These experiments were repeated for a number of phantoms having different values of $\delta\mu_a/\mu_{a0}$. In Figs. 4(b) and 4(c) the deviation μ_a-μ_a^{ref} of the absorption coefficient μ_a from the reference value of the slab μ_a^{ref}, as a function of μ_a^{ref} is plotted. For R_{imp}=10 mm the result shown in Fig. 4(b) indicates that in practice the limit for second order perturbation analysis lies at $\delta\mu_a/\mu_{a0}\approx 3$, with Λ=3.8. The situation is getting much worse as soon as one gets to an absorber radius of 15 mm. In this case, the perturbation theory can also be used still up to moderate values of $\delta\mu_a/\mu_{a0}\approx 1$ (Λ=2.9) from Fig. 4(c). For values of $\delta\mu_a/\mu_{a0}$ higher as roughly 3 and radii larger as 10 mm, Neumann series tends to converge to a wrong limit, as it can be seen from Figs. 4(b) and 4(c).

At the next refinement stage the third order perturbation theory was used. The were no observable improvements of the second order level up to sphere radii of 15 mm and absorption values μ_a up to 0.15 cm^{-1}, see Figs. 4(a)–4(c). Slight (7%) improvement of strongly diverging values at absorption levels μ_a=0.18 cm^{-1} do not save the failure of the perturbation model in this extreme limit.

In any case a conclusion can be drawn that the second order perturbation method competes with Padé approximants for moderate $\delta\mu_a/\mu_{a0}\approx 1$ and tumor radii $R>10$ mm [Fig 4(a)]. In fact the analytic form of the Padé approximation is equivalent to the expression derived by Xu *et al.* [21] in the frequency domain for the nonlinear multiple passage effect. The authors obtain the nonlinear correction factor $NCF=[1+\bar{N}_{self}(\omega;R)V\delta\mu_a(\vec{r})]^{-1}$ with $\bar{N}_{self}(\omega;R)$ being the self-propagator giving the probability of a photon to revisit volume V, and ω—the modulation frequency of light. This approximation, however, is valid only for the cases of absorber being far from detector and source, and for sizes much smaller than the distances to the source and detector. In addition, stronger deviations for inclusions with reduced absorption or scattering (cysts with $0>\delta\mu_s'/\mu_{s0}'>-1$) is expected, due to the strong nonlinearity at high transmissions and condition $\mu_a>0$ ($\mu_s'>0$).

It can be concluded in general, that PDW is the only method discussed which adequately reproduces the experimental values for tumors with $\delta\mu_a/\mu_{a0}$ up to at least ≈ 4 independent of the size of the lesion. Unfortunately, in addition to the size, target location and shape limits mentioned in the Introduction, the accessible CPU speed is far away to use the PDW method for online imaging. In contrast, the second order perturbation method, accurate enough for tumors with $\delta\mu_a/\mu_{a0}<3$ and sizes $R<15$ mm, is delivering values of optical coefficients within CPU times of less than 1 min (PC AMD Athlon XP Processor, 1.5 GHz). In the validity range its accuracy sometimes even exceeds the performance of the PDW method.

IV. CONCLUSION

Explicit formulas have been developed for higher order perturbation treatment in the studies of diffuse light propagation in tissue. Their application to the published experiments on absorbing phantoms demonstrated that the inclu-

sion of the second order correction significantly improves the accuracy of the desired optical parameters in the range of $\delta\mu_a/\mu_{a0} \leqslant 3$ ($\mu_{a0}=0.04$ cm^{-1}, $\mu'_{s0}=10$ cm^{-1}) and lesion radii up to 15 mm. In some cases ($\delta\mu_a/\mu_{a0} \leqslant 1$, $R=10$ mm) its accuracy competes with the PDW method and Padé approximants. However, PDW is the only method discussed in the paper, working practically as equally well for all values of absorption and tumor sizes in question. The inclusion of a third perturbation order is not introducing any notable change. The obtained formulas can be used for better quality of online data analysis in optical mammography.

The accuracy limitation $\delta\mu_a/\mu_{a0} \leqslant 1$ for $R > 10$ mm for the currently used in practice empiric method of Padé approximants was concluded by comparison with results delivered by the second and third order perturbation theory.

A dimensionless characteristic parameter Λ, depending on the amplitude of perturbation, tumor size, and background scattering coefficient suggested one should quantify the limits of perturbation theory. Its value in the validity regions should not strongly exceed $\Lambda=3$. The remarkable property of Λ being exactly twice the index of the exponential correction factor in the random walk theory points at the commonality between both theories.

The general expression for the absorptive perturbation correction of arbitrary order is developed and can be compared to other existing theories, such as the Born approximation to radiative transfer equations and empiric Padé approximants.

Detailed analysis of the singular behavior of the Born series shows the reliability of the solution for absorptive perturbations up to the arbitrary order. The limitation on the second order scattering solution at short distances ("self-interacting" terms) due to the breakdown of the diffusion approximation can be removed by use of the simplified solution to the radiative transfer equation. A number of measurements on purely scattering phantoms are desired to resolve the role of the ballistic contribution in the higher order scattering and saturation effects at high transmissions.

The derivation of the given formalism in the reflection geometry as well as in the frequency domain can be viewed as a next step to meet the needs of clinical research.

An alternative application of the developed higher order formalism to the linear perturbation model for several inclusions is suggested. Impressive sensitivity to the depth difference is demonstrated, with the time reversibility of perturbation solution being satisfied. The ultimate goal can be certainly achieved only by tests on phantoms and in the *in vivo* measurements.

ACKNOWLEDGMENTS

The author is indebted to Dr. A. Kummrow, PTB-Berlin, Professor F. von Oppen, Professor H. Begehr, FU Berlin, and Professor J.R. Manson, Clemson University, SC, USA for fruitful discussions. Support from SFB 290, Free University of Berlin, and use of the supercomputer facilities of Konrad-Zuse Center, Berlin are greatly acknowledged.

APPENDIX A

Briefly summarizing the *first order* expressions given in Refs. [5,9] the *absorption* expressed in current notations reads

$$J^{\alpha\gamma(1)}_{m,k_{abs}}(x,y,d,t) = -\delta\mu_a \frac{\exp(-\mu_{a0}vt)}{(4\pi)^{5/2}D_0{}^{3/2}v^{1/2}t^{3/2}} \int_{V_q} \frac{z^\alpha_m}{(r^\alpha_m)^2} \times \left[\frac{1}{r^\alpha_m} + \frac{(r^+_{qm})^2}{r^\gamma_{qk}(2D_0vt)}\right] \exp\left[-\frac{(r^+_{qm})^2}{4D_0vt}\right] dV_q. \tag{A1}$$

The *scattering* in its turn

$$J^{\alpha\gamma(1)}_{m,k_{scat}}(x,y,d,t) = -\delta D \frac{\exp(-\mu_{a0}vt)}{2(4\pi)^{5/2}D_0{}^{5/2}v^{3/2}t^{5/2}} \int_{V_q} \left\{ \frac{(-1)^\alpha z^\gamma_{qk} r^+_{qm}}{(r^\times_{qm})^2}\left[\frac{(r^-_{qm})^2}{r^\times_{qm}} + 1 + \frac{(r^+_{qm})^2}{2D_0vt}\right] - \frac{\vec{r}^{\,*}_{qm} z^\alpha_m}{(r^\alpha_m)^3}\left\{\frac{3}{(r^\alpha_m)^2} - \frac{(r^+_{qm})^2[2r^\times_{qm} - 3(r^\gamma_{qk})^2 - (r^\alpha_m)^2]}{r^\alpha_m (r^\gamma_{qk})^3 (2D_0vt)} + \frac{(r^+_{qm})^4}{(r^\gamma_{qk}2D_0vt)^2}\right\}\right\} \exp\left[-\frac{(r^+_{qm})^2}{4D_0vt}\right] dV_q \tag{A2}$$

with $r^\pm_{qm} = r^\alpha_m \pm r^\gamma_{qk}$; $r^\times_{qm} = r^\alpha_m \cdot r^\gamma_{qk}$; $\vec{r}^{\,*}_{qm} = \vec{r}^{\,*\alpha}_m \cdot \vec{r}^{\,\gamma}_{qk}$. The final expression for the *second order absorption* correction, as stated in Eq. (15), is shown to be

$$J^{\alpha\beta\gamma(2)}_{m,n,k_{abs-abs}}(x,y,d,t) = (\delta\mu_a)^2 \frac{\exp(-\mu_{a0}vt)}{(4\pi)^{7/2}D_0{}^{5/2}v^{1/2}t^{3/2}} \int_{V_p}\int_{V_q} \frac{z^\alpha_m}{(r^\alpha_m)^2 r^\times_{pq}}\left[\frac{r^+_{pq}}{r^\alpha_m} + \frac{r^2_{pqm}}{(2D_0vt)}\right] \exp\left[-\frac{r^2_{pqm}}{4D_0vt}\right] dV_p dV_q. \tag{A3}$$

The notations for the distances used in (A3) are read as follows:

$$r^\pm_{pq} = r^\beta_{pn} \pm r^\gamma_{qk}; \quad r_{pqm} = r^+_{pq} + r^\alpha_m; \quad r^\times_{pq} = r^\beta_{pn} \cdot r^\gamma_{qk}.$$

The coupling of *absorption to scattering* formulated by Eq. (17) reduces to

$$J^{\alpha\beta\gamma^{(2)}}_{m,n,k_{abs-scat}}(x,y,d,t) = \delta\mu_a \delta D \frac{\exp(-\mu_{a0} v t)}{(4\pi)^{7/2} D_0{}^{5/2} v^{1/2} t^{3/2}} \int_{V_p}\int_{V_q} \frac{\overleftrightarrow{r}^*_{pq} z^\alpha_m r_{pqm}}{r^\alpha_m (r^\times_{pq})^2 r^+_{pq}} \left\{ \left\{ g \cdot \left[\frac{2r^\alpha_m - r_{pqm}}{(r^\alpha_m)^2} - \frac{1}{r^+_{pq}} \right] + \frac{3}{r_{pqm}} - \frac{3}{r^+_{pq}} \right\} \frac{1}{2D_0 v t} \right.$$
$$\left. - \left[g \frac{r^2_{pqm}}{r^\alpha_m} - \frac{r^+_{pq}(3r_{pqm} r^\alpha_m - r^2_{pqm})}{(r^\alpha_m)^2} + 3r_{pqm} \right] \frac{1}{(2D_0 v t)^2} - \frac{r^3_{pqm} r^+_{pq}}{r^\alpha_m (2D_0 v t)^3} \right\}$$
$$\times \exp\left[- \frac{r^2_{pqm}}{4D_0 v t} \right] dV_p dV_q \tag{A4}$$

with $g = \frac{(r^-_{pq})^2}{r^\times_{pq}} + 1$; and $\overleftrightarrow{r}^*_{pq} = \vec{r}^{*\beta}_{pn} \cdot \vec{r}^\gamma_{qk}$.

The complementary term of *the scattering to absorption* [Eq. (20)] coupling looks a little bit more complicated

$$J^{\alpha\beta\gamma^{(2)}}_{m,n,k_{scat-abs}}(x,y,d,t)$$
$$= \delta\mu_a \delta D \frac{\exp(-\mu_{a0} v t)}{(4\pi)^{7/2} D_0{}^{5/2} v^{1/2} t^{3/2}} \int_{V_p}\int_{V_q} \left[f'_1 + f'_2 \right.$$
$$\left. - \frac{z^\alpha_m}{r^\alpha_m}(f_1 + f_2)\left(\frac{2}{r^\alpha_m} + \frac{r_{pqm}}{2D_0 v t} \right) \right] \frac{\exp\left[- \frac{r^2_{pqm}}{4D_0 v t} \right]}{(r^\alpha_m)^2} dV_p dV_q, \tag{A5}$$

where

$$f_1 = \frac{\overleftrightarrow{r}^*_{pm}}{(r^\beta_{pn})^3} \left[\frac{1}{r^\alpha_m} + \frac{r^2_{pqm}}{(2D_0 v t) r^+_{pq}} \right],$$

$$f'_1 = \frac{\partial f_1}{\partial z} = \frac{(-1)^\alpha z^\beta_{pn}}{(r^\beta_{pn})^3} \left[\frac{1}{r^\alpha_m} + \frac{r^2_{pqm}}{(2D_0 v t) r^+_{pq}} \right]$$
$$+ \frac{\overleftrightarrow{r}^*_{pm}}{(r^\beta_{pn})^3} \left[- \frac{1}{(r^\alpha_m)^2} + \frac{r_{pqm}}{(D_0 v t) r^+_{pq}} \right] \frac{z^\alpha_m}{r^\alpha_m};$$

and $f_2 = F_1 F_2$, $f'_2 = \partial f_2 / \partial z = F'_1 F_2 + F_1 F'_2$ with

$$F_1 = \frac{\overleftrightarrow{r}^*_{pm} r_{pqm}}{(2D_0 v t) r^\beta_{pn} r^\times_{pq}};$$

$$F_2 = \frac{(r^\alpha_m - r^+_{pq})^2}{r^\alpha_m r^+_{pq}} + 1 + \frac{r^2_{pqm}}{2D_0 v t};$$

$$F'_1 = \frac{\partial F_1}{\partial z} = \left[\frac{z^\beta_{pn}(-1)^\alpha r_{pqm}}{r^\beta_{pn}} + \frac{\overleftrightarrow{r}^*_{pm}}{r^\beta_{pn}} \frac{z^\alpha_m}{r^\alpha_m} \right] \Big/ (r^\times_{pq} 2D_0 v t);$$

$$F'_2 = \frac{\partial F_2}{\partial z} = \left[\frac{(r^\alpha_m - r^+_{pq})}{(r^\alpha_m)^2 r^+_{pq}} + \frac{1}{D_0 v t} \right] \frac{r_{pqm} z^\alpha_m}{r^\alpha_m}.$$

The final expression for the *second order scattering* contribution [Eq. (22)] is the most space consuming

$$J^{\alpha\beta\gamma^{(2)}}_{m,n,k_{scat-scat}}(x,y,d,t)$$
$$= -(\delta D)^2 \frac{\exp(-\mu_{a0} v t)}{4(4\pi D_0)^{7/2} v^{3/2} t^{5/2}} \int_{V_p}\int_{V_q} \left[\frac{\overleftrightarrow{r}^*_{pq}}{(r^\beta_{pn})^3} (J^1_1 + J^2_1) \right.$$
$$\left. + \frac{2r^+_{pq}}{r^{\times 2}_{pq}} (J^1_2 + J^2_2) \right] \exp\left[- \frac{r^2_{pqm}}{4D_0 v t} \right] dV_p dV_q, \tag{A6}$$

where

$$J^1_1 = (-1)^\alpha 2 z^\beta_{pn} \left\{ \frac{3r_{pqm}}{(r^\beta_{pn} r^\alpha_m r^+_{pq})^2} F_2 - \frac{f_3}{(r^\gamma_{qk})^3 r^\beta_{pn} r^+_{pq}} F_3(r^+_{pq}, r^\alpha_m) \right.$$
$$\left. + \frac{1}{(r^\gamma_{qk})^2} \left\{ \frac{15}{(r^+_{pq})^3} + \frac{15 r_{pqm}}{(r^+_{pq})^2 2D_0 v t} - \frac{r^3_{pqm}[3r^+_{pq} r^\alpha_m - 6(r^\alpha_m)^2 - (r^+_{pq})^2]}{(r^\alpha_m)^3 r^+_{pq} (2D_0 v t)^2} + \frac{r^5_{pqm}}{(r^\alpha_m)^2 (D_0 v t)^3} \right\} \right\},$$

$$J^2_1 = - z^\alpha_m \overleftrightarrow{r}^*_{pm} \left\{ \frac{6}{(r^\beta_{pn})^2 (r^\alpha_m)^3} F_3(r^\alpha_m, r^+_{pq}) - \frac{f_3 r_{pqm}}{(r^\gamma_{qk} r^\alpha_m)^3 r^\beta_{pn} r^+_{pq} D_0 v t} F_4 + \frac{(r^+_{pq})^3}{(r^\gamma_{qk})^2 D_0 v t} \right.$$
$$\times \left\{ \frac{15}{(r^+_{pq})^6} + \frac{3r^2_{pqm}[3(r^+_{pq} r^\alpha_m)^2 - 4r^+_{pq}(r^\alpha_m)^3 - 2(r^+_{pq})^3 r^\alpha_m + 5(r^\alpha_m)^4 + (r^+_{pq})^4]}{2D_0 v t (r^\alpha_m r^+_{pq})^5} \right.$$
$$\left. \left. - \frac{3r^4_{pqm}[2r^+_{pq} r^\alpha_m - 2(r^\alpha_m)^2 - (r^+_{pq})^2]}{(r^\alpha_m r^+_{pq})^4 (2D_0 v t)^2} + \frac{r^6_{pqm}}{(r^\alpha_m r^+_{pq} 2D_0 v t)^3} \right\} \right\},$$

$$J_2^1 = (-1)^{\alpha+\beta+1} z_{qk}^{\gamma} \left[g \frac{r_{pqm}}{(r_m^{\alpha} r_{pq}^{+})^2} F_2 + \frac{1}{r_{pq}^{+}} F_3(r_{pq}^{+}, r_m^{\alpha}) \right],$$

$$J_2^2 = \frac{\vec{r}_{qm}^{**} z_m^{\alpha}}{r_m^{\alpha 3}} \left[g F_3(r_m^{\alpha}, r_{pq}^{+}) + \frac{r_{pqm}}{2 D_0 v t r_{pq}^{+}} F_4 \right],$$

with $f_3 = 2r_{pq}^{\times} - 3(r_{qk}^{\gamma})^2 - (r_{pn}^{\beta})^2$ and

$$F_3(a,b) = \left[\frac{3}{a^2} - \frac{r_{pqm}^2 (2ab - 3b^2 - a^2)}{(2D_0 v t) b^3 a} + \frac{r_{pqm}^4}{(2D_0 v t b)^2} \right];$$

$$F_4 = 3 \left[\left(\frac{r_m^{\alpha}}{r_{pq}^{+}} \right)^2 - \frac{r_m^{\alpha}}{r_{pq}^{+}} + 1 - \frac{r_{pq}^{+}}{r_m^{\alpha}} + \left(\frac{r_{pq}^{+}}{r_m^{\alpha}} \right)^2 \right] - \frac{r_{pqm}^2 [4 r_{pq}^{+} r_m^{\alpha} - 3(r_{pq}^{+})^2 - (3 r_m^{\alpha})^2]}{(2D_0 v t) r_m^{\alpha} r_{pq}^{+}} + \frac{r_{pqm}^4}{(2D_0 v t)^2}.$$

APPENDIX B

Time integrals to be taken in the expressions (15), (17), (20), and (22) are of the type

$$Int\left(\frac{n}{2}, \frac{m}{2}\right) = \int_0^t \frac{\exp\left[-\frac{A^2}{(t-t_p)} - \frac{B^2}{t_p} \right]}{(t-t_p)^{n/2} t_p^{m/2}} dt_p \tag{B1}$$

with A, B constants and n, m integers. For the case $n=m=3/2$ the integral can be easily obtained by using the convolution theorem and the answer can be found in Ref. [9],

$$Int\left(\frac{3}{2}, \frac{3}{2}\right) = \frac{\sqrt{\pi}}{t^{3/2}} \left(\frac{1}{A} + \frac{1}{B} \right) \exp\left[-\frac{(A+B)^2}{t} \right]. \tag{B2}$$

The integrals of higher orders are obtained through recursive parametric differentiation of (B2)

$$Int\left(\frac{3}{2} + i, \frac{3}{2} + j\right) = \frac{1}{(-2A)^i (-2B)^j} \frac{\partial^{i+j}}{\partial^i A \partial^j B} Int\left(\frac{3}{2}, \frac{3}{2}\right) \tag{B3}$$

with $i=0,\ldots,n-3$ and $j=0,\ldots,m-3$ to fit the definition (B1). The ordering of the differentiation can be permuted to check the validity of the results.

APPENDIX C

Every integral $I_{p,p-1}$, written again in Cartesian components, can be converted by using the arithmetic-geometric inequality to

$$\begin{aligned} I_{p,p-1} &= \int_V \frac{dV_p}{|\vec{r}_{p+1} - \vec{r}_p||\vec{r}_p - \vec{r}_{p-1}|} \\ &\leqslant \frac{1}{3} \prod_{i=1}^{3} \int \frac{dx_{p,i}}{\sqrt[3]{|x_{p+1,i} - x_{p,i}||x_{p,i} - x_{p-1,i}|}} \\ &\leqslant \frac{C'}{3} \prod_{i=1}^{3} |x_{p+1,i} - x_{p-1,i}|^{1/3}, \end{aligned} \tag{C1}$$

where C' is a constant.

Using the expressions given in the discussion of kernel iteration procedure, Ref. [18], one arrives in nth order at

$$I_{p,p-1} \leqslant \frac{C'}{3} \prod_{i=1}^{3} \int \int dx_{\mathrm{det},i} dx_{s,i} \frac{|x_{n,i} - x_{1,i}|^{2n/3-1}}{\sqrt[3]{|x_{\mathrm{det},i} - x_{n,i}||x_{1,i} - x_{s,i}|}}, \tag{C2}$$

where $x_{\mathrm{det},i}$ and $x_{s,i}$ are the coordinates of the detector and source, respectively. By substituting the n-dependent term by its maximum value $(2\varepsilon)^{2n/3}$ for each of three Cartesian components and taking it out of the integral, one finally obtains $I_{p,p-1} \leqslant C(2\varepsilon)^{2n}$, with

$$C = \frac{C'}{3} \prod_{i=1}^{3} \int \int \frac{dx_{\mathrm{det},i} dx_{s,i}}{\sqrt[3]{|x_{\mathrm{det},i} - x_{n,i}||x_{1,i} - x_{s,i}|}} \tag{C3}$$

and ε–voxel radius.

[1] D. Grosenick, H. Wabnitz, and H. H. Rinneberg, K. T. Moesta, and P. M. Schlag, Appl. Opt. **38**, 2927 (1999).
[2] D. Grosenick, B. Wassermann, R. Macdonald, H. Rinneberg, A. Torricelli, L. Spinelli, and R. Cubeddu, Proc. SPIE **5859**, 58590M (2005).
[3] V. Chernomordik, D. W. Hattery, and A. Ganjbakche, Opt. Lett. **25**, 951 (2000); V. Chernomordik, D. W. Hattery, D. Grosenick, H. Wabnitz, H. Rinneberg, K. T. Moesta, P. M. Schlag, and A. Ganjbakche, J. Biomed. Opt. **7**, 80 (2002).
[4] J. C. Hebden and S. R. Arridge, Appl. Opt. **35**, 788 (1996).
[5] S. Carraresi, T. S. M. Shatir, F. Martelli, and G. Zaccanti, Appl. Opt. **40**, 4622 (2001).
[6] S. R. Arridge, Appl. Opt. **34**, 7395 (1995).
[7] S. R. Arridge, P. van der Zee, M. Cope, and D. T. Delpy, Proc. SPIE **1431**, 204 (1991).
[8] M. R. Ostermeyer, J. Opt. Soc. Am. A **14**, 251 (1997).
[9] M. Morin, S. Verreault, A. Mailloux, J. Frechette, S. Chatingy, Y. Painchaud, and P. Beaudry, Appl. Opt. **39**, 2840 (2000); M. Morin, S. Chatingy, A. Mailloux, Y. Painchaud, and P. Beaudry, Proc. SPIE **3597**, 67 (1999).
[10] A. Torricelli, L. Spinelli, A. Pifferi, P. Taroni, and R. Cubeddu, Opt. Express **11**, 853 (2003).
[11] L. Spinelli, A. Torircelli, A. Pifferi, P. Taroni, and R. Cubeddu, Appl. Opt. **42**, 3145 (2003).
[12] D. Grosenick, H. Wabnitz, and H. Rinneberg, Proc. SPIE **2626**, 206 (1995).
[13] S. De Nicola, R. Esposito, and M. Lepore, Phys. Rev. E **68**, 021901 (2003).
[14] M. Bassani, F. Martelli, G. Zaccanti, and D. Contini, Opt. Lett. **22**, 853 (1997).

[15] G. Arfken, *Mathematical Methods for Physicists* (Academic Press, New York, 1970) Chapt. 16, pp. 737–738.
[16] M. S. Patterson, B. Chance, and B. C. Wilson, Appl. Opt. **28**, 2331 (1989).
[17] D. Contini, F. Martelli, and G. Zaccanti, Appl. Opt. **36**, 4587 (1997).
[18] P. M. Morse and H. Feshbach, *Methods of Theoretical Physics*, (McGraw-Hill, New York, 1953) pp. 922–925.
[19] M. Xu, W. Cai, M. Lax, and R. R. Alfano, Opt. Lett. **26**, 1066 (2001).
[20] D. Grosenick, H. Wabnitz, K. T. Moesta, J. Mucke, M. Möller, C. Stroszcynski, J. Stößel, B. Wassermann, P. M. Schlag, and H. H. Rinneberg, Phys. Med. Biol. **49**, 1165 (2004).
[21] M. Xu, W. Cai, and R. R. Alfano, Opt. Lett. **29**, 1757 (2004).